nature nanotechnology
SUPPLEMENTARY INFORMATION
DOI: 10.1038/NNANO.2012.112

Piezoelectric Nanoribbons for Monitoring Cellular Deformations

Thanh D. Nguyen, Nikhil Deshmukh, John M. Nagarah, Tal Kramer, Prashant K. Purohit, Michael J. Berry, Michael C. McAlpine

Supplementary Figures

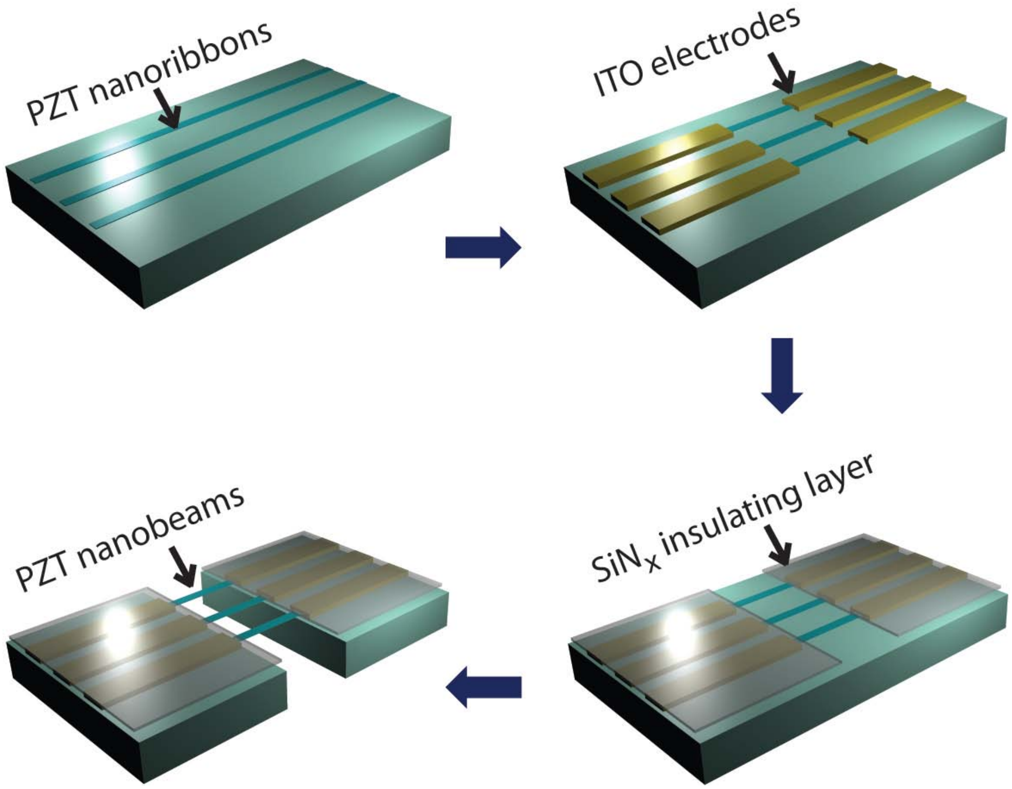

Supplementary Figure S1. Schematic of PZT nanoribbon and nanobeam fabrication process. PZT nanoribbons were patterned on a MgO substrate via lift-off. ITO electrodes were then patterned on the nanoribbons. SiN_x was deposited to coat the electrodes, but not the exposed PZT nanoribbons. Phosphoric acid was finally used to undercut-etch the MgO substrate, thereby suspending the PZT nanoribbons.

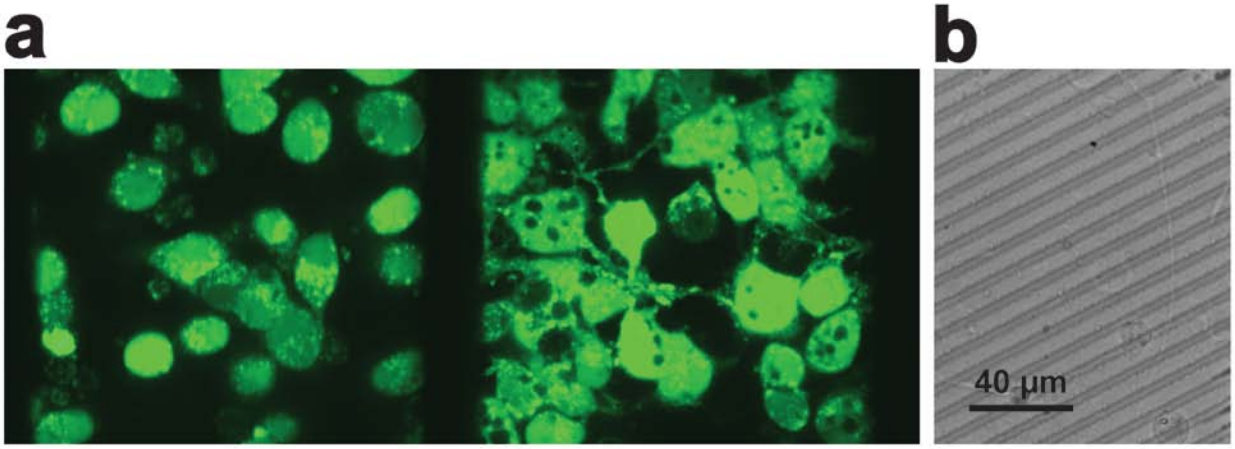

Supplementary Figure S2. Cell viability tests. a. Cells cultured on PZT nanoribbons at various locations show primarily green fluorescence – an indicator of cell health. **b.** Optical image shows differentiated cells with long, healthy neurites when cultured on PZT nanoribbons.

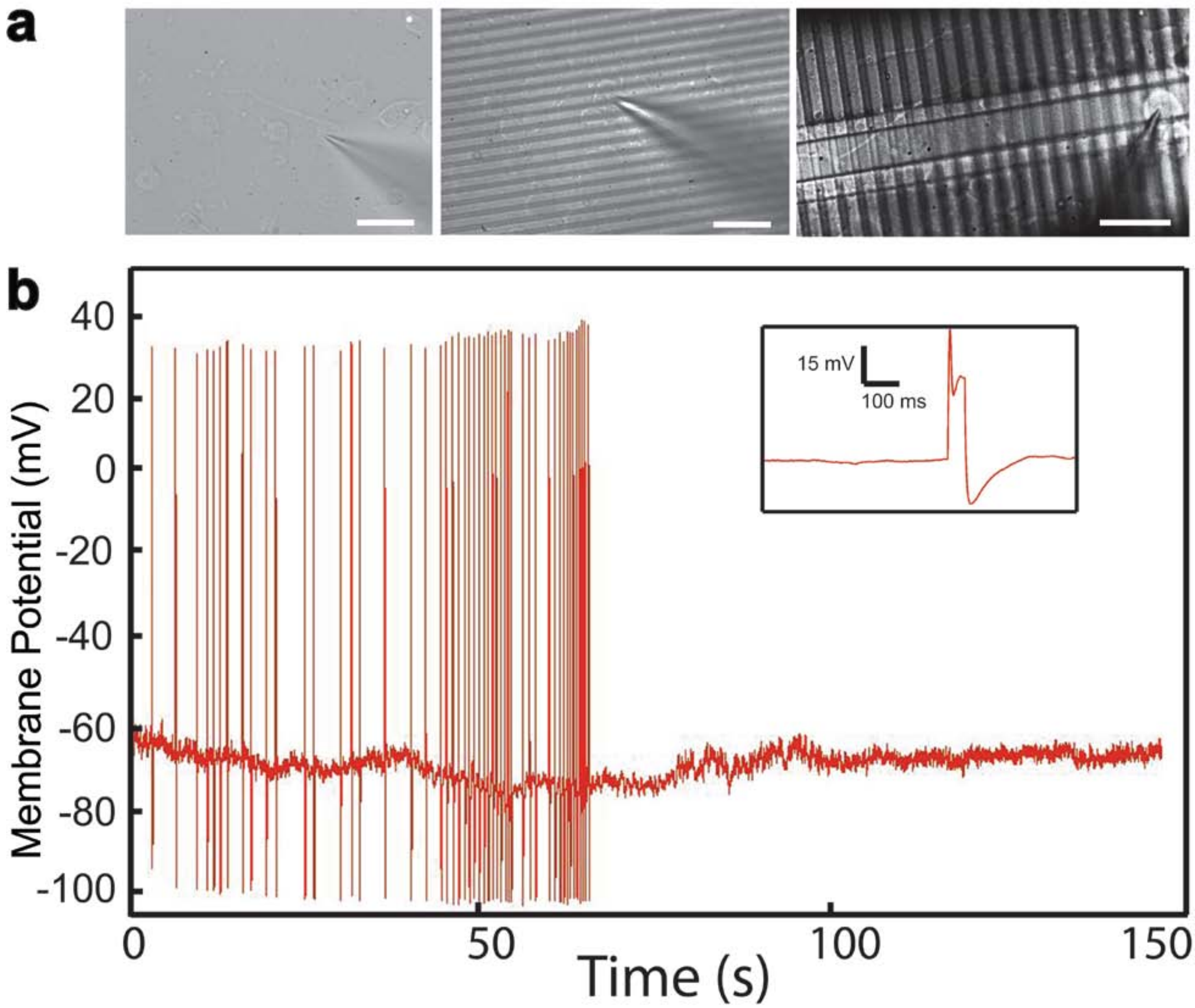

Supplementary Figure S3. Electrophysiological behavior of PC12 cells. a. From left to right: patch-clamp recording of PC12 on a PZT thin film, on PZT nanoribbons, and on suspended PZT nanoribbons (scale bars are 40 µm for all images). **b.** A typical stimulus-evoked action potential of PC12 on PZT nanoribbons. Similar behavior was seen in cells cultured on PZT films and suspended PZT nanoribbons.

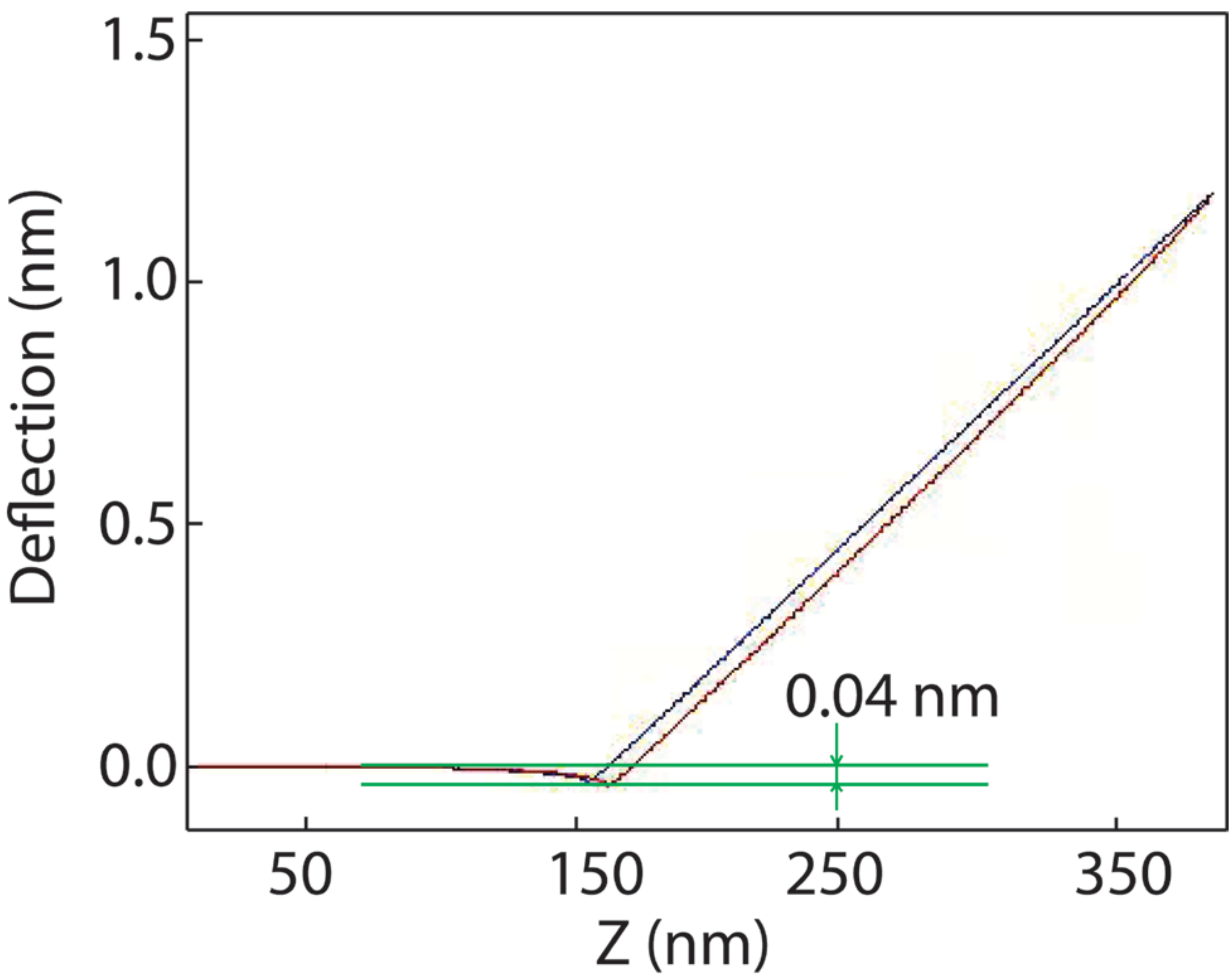

Supplementary Figure S4. AFM force curve. A typical force-curve of an AFM tip was collected in ramping mode. The spring constant k ~ 38 ± 7 N/m was identified via thermal tune. The applied force of the AFM tip on PZT nanobeams was calculated as $F = k * \Delta x$, where Δx is the sudden deflection of the AFM tip (~0.04 nm) when it descends to the surface of the PZT nanobeams. Using different AFM tips with different spring constants, minute differential forces can be applied on the PZT nanobeams as seen in Figure 3c of the main text.

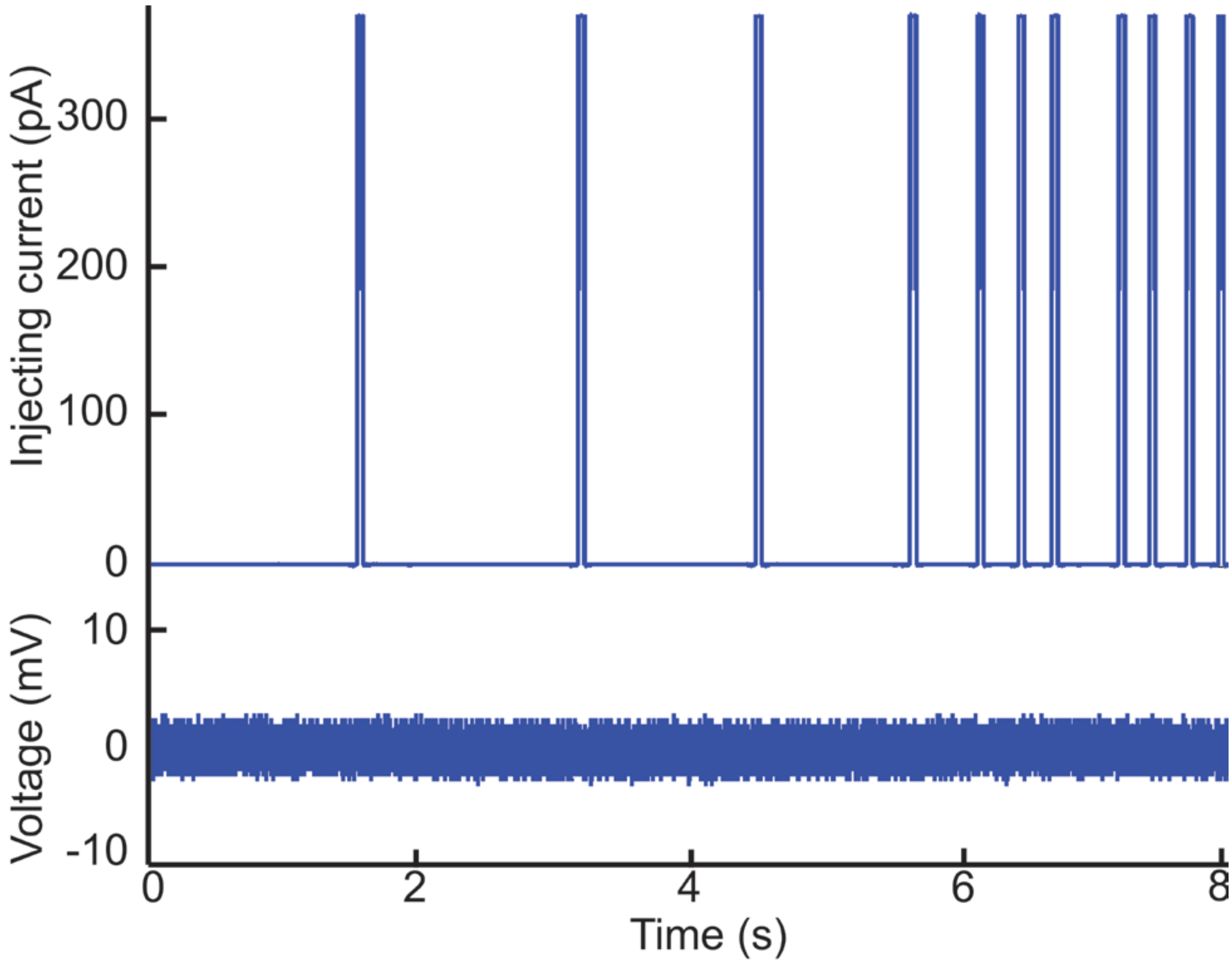

Supplementary Figure S5. Patch-clamp control experiment. In this experiment, the pipette tip was used to inject current on the PZT nanoribbons without the presence of cells. The upper trace is the injecting current from the pipette, while the lower trace is the PZT response, which shows no discernible signal.

Supplementary Methods

In our experiments the cells are patch clamped to induce depolarization and they rest on PZT nanobeams so that a change in radius of the cell causes a deflection of the beam, which in turn can be easily detected because the piezoelectric properties of PZT lead to the generation of a voltage upon bending. Our goal is to analyze these experiements so as to be able to predict the change in shape of the cells in response to membrane depolarization.

Model for voltage dependent membrane tension

The surface tension σ in a single leaflet of lipid bilayer membrane is controlled by the Lippmann equation which dictates that

$$\sigma = \sigma_0 - \frac{1}{2} C_D V_s^2, \tag{1}$$

where σ_0 is the voltage independent tension, C_D is the specific capacitance of the electric double layer (or cloud of ions) next to the leaflet, and V_s is the surface potential at the leaflet [S1]. This surface potential and the distribution of ions in the electric double layer is governed by the Poisson-Boltzmann equation [S2]. From the solution to the fully non-linear Poisson-Boltzmann equation near a surface with charge density q it can be shown that

$$V_s = \frac{2k_B T}{e} \sinh^{-1}\left(\frac{q}{2\sqrt{2c\epsilon_w \epsilon_0 k_B T}}\right), \tag{2}$$

where c is the ionic strength of the solution far away from the surface, ϵ_w is the relative perimittivity of water, ϵ_0 is the permittivity of vaccuum and $k_B T$ is the thermal energy scale and we have assumed that both positive and negative ions of valence 1 are present in the solution. This equation and (1) can then be applied to both the interior and exterior leaflets of the membrane and the surface tension in both can be added to give the surface tension τ in the cell-membrane. The result is:

$$\frac{(\tau - \tau_I)e}{\sqrt{(2k_B T)^3 \epsilon_w \epsilon_0}} = \sqrt{c_{ext}}\left[\sinh^{-1}\left(\frac{q_{ext} - C_m V}{2\sqrt{2c_{ext}\epsilon_w \epsilon_0 k_B T}}\right)\right]^2 + \sqrt{c_{int}}\left[\sinh^{-1}\left(\frac{q_{int} + C_m V}{2\sqrt{2c_{int}\epsilon_w \epsilon_0 k_B T}}\right)\right]^2, \tag{3}$$

where C_m is the capacitance of the lipid bilayer (assumed much larger than C_D on both the interior and exterior), V is the applied potential through the patch clamp and τ_I is a voltage independent tension. q_{int} and q_{ext} are the charge densities on the interior and exterior leaflets of the cell membrane and have to be treated as fitting parameters along with C_m and τ_I. But, appropriate values for these parameters are available from earlier work [S1].

Using the Young-Laplace law

In this section we will assume for simplicity that the cell remains spherical and demonstrate how a change in voltage through the patch-clamp results in a force exerted by the cell on

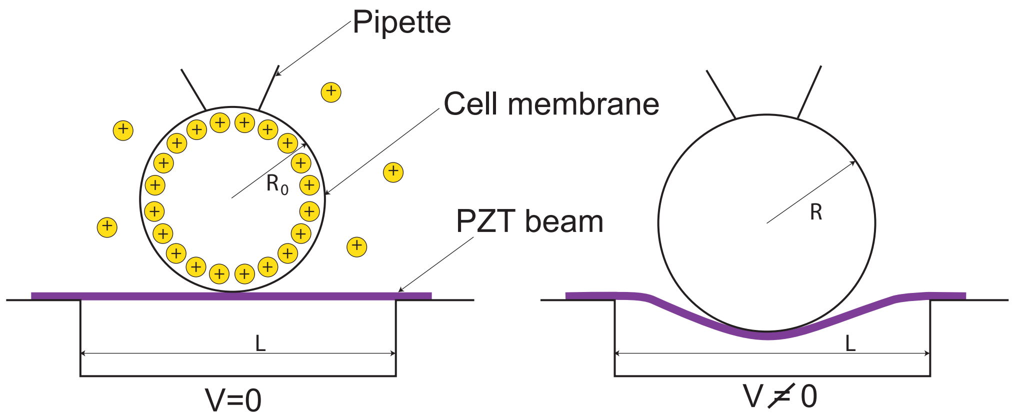

Figure 1: A cell 'patch-clamped' using a pipette. The potential difference between the interior and exterior of the cell can be changed using the patch clamp technique. There are ions both inside and outside the cell as shown in the left panel. The ions interact with opposite charges on the membrane and with each other to induce a tension in the membrane. The membrane tension can be changed by artificially changing the potential difference between the inside and outside of the cell. This causes a change in shape of the cell which can be detected by the deflection of the PZT beam as shown in the right panel. Here we assume for simplicity that the cell remains spherical. The more realistic case is treated later.

the substrate. Once the surface tension τ in the cell membrane is known in terms of the applied voltage V we can apply the Young-Laplace law to calculate how its shape changes. This law states that the pressure difference p between the interior and exterior of the cell is related to the surface tension and local mean curvature on the cell membrane through

$$p = \tau \left(\frac{1}{R_m} + \frac{1}{R_p} \right), \tag{4}$$

where R_m is the meridional (principal) curvature and R_p is the principal curvature along lines perpendicular to the meridians. We have, of course, assumed here that the cell membrane has an axisymmetric shape, which is good for the geometry of our experiments. Note that p remains constant even though the cell shape changes since the concentrations c_{int} and c_{ext} of ions are realistically assumed not to change when the cell is electrically and mechanically manipulated since they are controlled by regulation of ion channels by the cell. The Young-Laplace law (which is a statement of local mechanical equilibrium) and the boundary conditions imposed by the pipette and the PZT beam are sufficient to calculate the shape of the cell for some applied voltage V. The final expressions for the shape of the cell are in terms of elliptic functions as shown by Lin and Freund [S3] in a different context.

In order to illustrate how the general framework given above can be applied we will illustrate it by assuming that the cell remains spherical even after the tension in the cell membrane changes (see figure 1). Let us assume that at the resting state of a cell when $V = 0$ the membrane tension is τ_0, the radius of the cell is R_0 and the pressure difference is p. Then the Young-Laplace law gives $\frac{2\tau_0}{R_0} = p$. When $V \neq 0$ the cell's radius changes to R and the tension τ is given by eqn.(3). The PZT beam deflects by an amount $\delta = 2(R - R_0)$

at the center. This provides a reaction $F = k\delta$ where k is a spring constant. For instance, $k = \frac{192EI}{L^3}$ for a clamped-clamped beam and $k = \frac{48EI}{L^3}$ for a hinged-hinged beam, where E is the Young's modulus of PZT, I is the moment of inertia of the cross-section of the PZT beam, and L is its length. Realistically, k should be determined from experiment since we expect manufacturing defects in the PZT beam that would result in $\frac{48EI}{L^3} \leq k \leq \frac{192EI}{L^3}$. Mechanical equilibrium at the equator of the spherical cell demands that

$$\frac{2\tau}{R} + \frac{F}{\pi R^2} = p = \frac{2\tau_0}{R_0}. \tag{5}$$

This equation can be solved immediately to give

$$R = R_0 \left[\frac{\tau}{2\tau_0} + \frac{k}{2\pi\tau_0} + \sqrt{\left(\frac{\tau}{2\tau_0} + \frac{k}{2\pi\tau_0} \right)^2 - \frac{k}{\pi\tau_0}} \right]. \tag{6}$$

This formula provides a good estimate of the actual radius of the cell in the limit when k is small. Clearly, when $k = 0$, meaning the PZT beam is absent, the Young-Laplace result is recovered. The force F exerted by the cell on the PZT beam due to the change in voltage V can be computed using $F = 2k(R - R_0)$. When k is large we have to resort to a more general method explained in the following.

Analysis of cells on stiff PZT beams

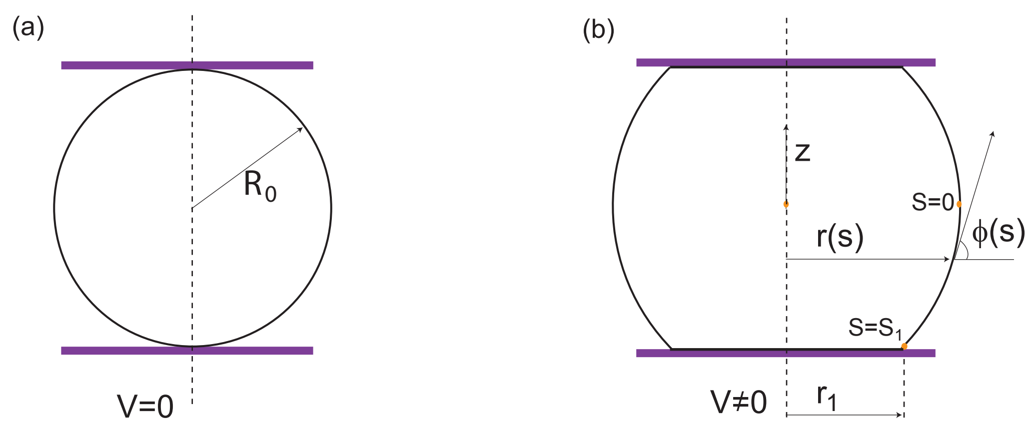

Figure 2: (a) Schematic diagram with the pipette and PZT beam replaced by planes. We assume that the pipette does not move and the PZT beam is much stiffer than the cell. The response of the cell resembles converse flexoelectricity – a potential difference causes a change in curvature of the cell membrane. (b) The change in membrane curvature causes a change in the shape of the cell. We assume that it remains axisymmetric about the vertical dashed line. The geometrical variables are indicated.

When the PZT beam on which the cell rests is stiff then it does not deflect much in response to the depolarization. We approximate the PZT beam as being infinitely stiff and directly compute the reaction force imposed by the beam on the cell. Let this force be F. Then if we make a cut perpendicular to the axis of the cell where the radius is $r(s)$ and the tangent angle to the contour of the axisymmetric shape is $\phi(s)$ (see figure 2) then equilibrium demands that

$$2\pi\tau r(s)\sin\phi(s) = \pi r^2(s)p - F. \tag{7}$$

We want to know F and $r(s)$ as a function of τ. When $\tau = \tau_0$, $F = 0$ and the cell is a sphere of radius R_0, so that by applying the above equation at the equator where $\phi = \frac{\pi}{2}$ we see that

$$p = \frac{2\tau_0}{R_0}. \tag{8}$$

When $\tau > \tau_0$ the cell tends to bulge but we will assume that the distance $2R_0$ between the pipette and the PZT beam changes by a negligible amount. This constraint is enforced by a force $F \neq 0$. In the experiments $2R_0$ is about $20\mu m$ and it changes by only a few nanometers when the cells are depolarized. So, our assumption that the distance between the pipette and the PZT beam does not change is justified. When $F \neq 0$ the cell is squished and it makes contact with the PZT beam over a circular region of radius r_1. The angle ϕ_1 at $r = r_1$ depends on the adhesion energy per unit area between the cell and the PZT beam. If the adhesion energy density is zero then the angle ϕ_1 is zero too. So, we have

$$\sin\phi_1 = \frac{pr_1}{2\tau} - \frac{F}{2\pi r_1 \tau} = 0 \tag{9}$$

which gives $r_1^2 = \frac{F}{\pi p}$. From geometry,

$$\frac{dr}{ds} = \cos\phi(s) = \sqrt{1 - \sin^2\phi(s)}, \qquad \frac{dz}{ds} = \sin\phi(s) \tag{10}$$

where $\sin\phi(s)$ is given by (7) in terms of $r(s)$ and F. We can therefore integrate the differential equation for $r(s)$ and get

$$r(s) = \frac{\sqrt{2}\tau}{p}\sqrt{1 + \frac{Fp}{2\pi\tau^2} + \sqrt{1 + \frac{Fp}{\pi\tau^2}}\cos\frac{ps}{\tau}}, \tag{11}$$

where $s = 0$ is taken to be at the equator of the cell. Let $s = s_1$ be such that $r(s_1) = r_1$ and $\phi(s_1) = \phi_1 = 0$. Using $r_1^2 = F/\pi p$ and (11) above it is easy to see that

$$\cos\frac{ps_1}{\tau} = \frac{-1}{\sqrt{1 + \frac{Fp}{\pi\tau^2}}}, \tag{12}$$

from which we get

$$s_1 = \frac{\tau}{p}\left(\pi + \cos^{-1}\frac{1}{\sqrt{1 + \frac{Fp}{\pi\tau^2}}}\right). \tag{13}$$

Integrating the equation for $z(s)$ we get

$$z(s) = \int_0^s \sin\phi(s)\,ds = \int_0^s \left(\frac{pr(s)}{2\tau} - \frac{F}{2\pi\tau r(s)}\right), \tag{14}$$

where $r(s)$ is given by (11) above. We substitute for $r(s)$ to get

$$\begin{aligned} z(s) &= \frac{1}{\sqrt{2}}\int_0^s \sqrt{1+\frac{Fp}{2\pi\tau^2}+\sqrt{1+\frac{Fp}{\pi\tau^2}}-2\sqrt{1+\frac{Fp}{\pi\tau^2}}\sin^2\frac{ps}{2\tau}}\,ds \\ &\quad -\frac{Fp}{2\sqrt{2}\pi\tau^2}\int_0^s \frac{ds}{\sqrt{1+\frac{Fp}{2\pi\tau^2}+\sqrt{1+\frac{Fp}{\pi\tau^2}}-2\sqrt{1+\frac{Fp}{\pi\tau^2}}\sin^2\frac{ps}{2\tau}}}. \end{aligned} \tag{15}$$

We take $s = s_1$ and reduce this expression to

$$z(s_1) = \frac{\tau}{p}\left(1+\sqrt{1+\frac{Fp}{\pi\tau^2}}\right)\int_0^{\frac{ps_1}{2\tau}} \sqrt{1-m^2\sin^2\theta}\,d\theta - \frac{F}{\pi\tau}\frac{1}{1+\sqrt{1+\frac{Fp}{\pi\tau^2}}}\int_0^{\frac{ps_1}{2\tau}}\frac{d\theta}{\sqrt{1-m^2\sin^2\theta}}, \tag{16}$$

where

$$m^2 = \frac{2\sqrt{1+\frac{Fp}{\pi\tau^2}}}{1+\frac{Fp}{2\pi\tau^2}+\sqrt{1+\frac{Fp}{\pi\tau^2}}} \leq 1, \tag{17}$$

and θ is a dummy variable. Recognizing the incomplete elliptic integrals above we write

$$z(s_1) = \frac{\tau}{p}\left(1+\sqrt{1+\frac{Fp}{\pi\tau^2}}\right)E(\theta_1|m) - \frac{F}{\pi\tau}\frac{1}{1+\sqrt{1+\frac{Fp}{\pi\tau^2}}}F(\theta_1|m), \tag{18}$$

where $E(x|k)$ is the incomplete elliptic integral of the second kind with modulus k and $F(x|k)$ is the incomplete elliptic integral of the first kind with modulus k and $\theta_1 = \frac{ps_1}{2\tau}$. The stiff PZT beams enforce the constraint that $z(s_1) = R_0$. For small values of $\frac{Fp}{\pi\tau^2}$ we see from (13) and (17) that $\theta_1 \approx \frac{\pi}{2}$ and $m^2 \approx 1$. Under these circumstances the second term involving $F(\theta_1|m)$ is much smaller than the first term involving $E(\theta_1|m)$, so we neglect the second term. Furthermore, $E(\theta_1|1) = \sin\theta_1$. We note that

$$\theta_1 = \frac{ps_1}{2\tau} = \frac{\pi}{2}+\frac{1}{2}\cos^{-1}\frac{1}{\sqrt{1+y}}, \qquad y = \frac{Fp}{\pi\tau^2} << 1. \tag{19}$$

So (18) becomes

$$\frac{pR_0}{\tau} \approx \left(1+\sqrt{1+y}\right)\sqrt{\frac{1+\frac{1}{\sqrt{1+y}}}{2}}, \qquad y << 1. \tag{20}$$

Expanding upto linear order in y we are left with

$$1+\frac{y}{8} = \frac{pR_0}{2\tau}, \tag{21}$$

which can be solved to get

$$y = \frac{Fp}{\pi\tau^2} = -8\left(1-\frac{pR_0}{2\tau}\right). \tag{22}$$

This gives the force exerted by the beam on the cell. The final formula for the force exerted by the *cell on the beam* is (note the change in sign of F):

$$F = \frac{8\pi\tau^2}{p}\left(1-\frac{R_0}{R}\right), \tag{23}$$

where

$$p = \frac{2\tau_0}{R_0}, \qquad R = \frac{2\tau}{p}, \tag{24}$$

and τ is given by (3). Clearly, $F > 0$ when $R > R_0$.

Pancake shaped cell

Cells on many substrates become pancake shaped. This suggests that there is an adhesive interaction between the cell and the substrate that results in a decrease of free energy by amount Γ per unit contact area. To account for the adhesive interactions we have to make some non-trivial modifications to the theory given in the previous section. The shape of the cell is still described by the same equation for $r(s)$ (eqn. (11)). But, the expression for s_1 becomes more complicated:

$$\cos\frac{ps_1}{\tau} = \frac{\frac{p^2r_1^2}{2\tau^2} - 1 - \frac{Fp}{2\pi\tau^2}}{\sqrt{1 + \frac{Fp}{\pi\tau^2}}}. \tag{25}$$

Here r_1 is the radius over which contact occurs between the cell and the substrate and it is no longer zero when $F = 0$ because of the adhesive interactions. The integral for $z(s)$ remains the same but $\frac{ps_1}{2\tau}$ appears in the limit of the integral where the expression for calculating s_1 is given above. The analysis to impose the constraint that the cell is confined between two fixed surfaces proceeds along the same lines as in the previous section. If the distance between the two confining surfaces is $2Z_0$ (see figure 3) then the equation to solve for F takes the form

$$Z_0 = \frac{\tau}{p}\left[1 + \sqrt{1 + \frac{Fp}{\pi\tau^2}}\right]\sin\frac{ps_1}{2\tau} = \frac{\tau}{p}\left[1 + \sqrt{1 + \frac{Fp}{\pi\tau^2}}\right]\sqrt{\frac{1 - \cos\frac{ps_1}{\tau}}{2}}, \tag{26}$$

where we can use (25) for $\cos\frac{ps_1}{\tau}$. When $\tau = \tau_0$, $F = 0$ and $r_1 = r_0$ the above equation yields

$$Z_0 = \frac{2\tau_0}{p}\sqrt{1 - \frac{pr_0^2}{4\tau_0^2}}. \tag{27}$$

Note that if $r_0 = 0$ when $\tau = \tau_0$ and $F = 0$ then the cell is a sphere and $Z_0 = R_0 = \frac{2\tau_0}{p}$, as expected. This is the case when $\Gamma = 0$. When $\Gamma \neq 0$ we have to determine the magnitude of Γ from the known pancake shape of the cell when $F = 0$. This is a difficult exercise in general, but in a certain limit it is possible to write some simple relations [S3]. In particular, the radius r_1 over which contact between the cell and the substrate occurs in this limit is given by [S3]:

$$r_1 = \frac{\Gamma}{p}\left[\sqrt{\frac{pR_0}{\Gamma} - \frac{F}{\pi R_0\Gamma} - 1} + \sqrt{\frac{pR_0}{\Gamma} - \frac{F}{\pi R_0\Gamma} + \frac{Fp}{\pi\Gamma^2} - 1}\right]. \tag{28}$$

When $F = 0$ and $\tau = \tau_0$ this reduces to

$$r_0 = \frac{2\Gamma}{p}\sqrt{\frac{pR_0}{\Gamma} - 1}, \tag{29}$$

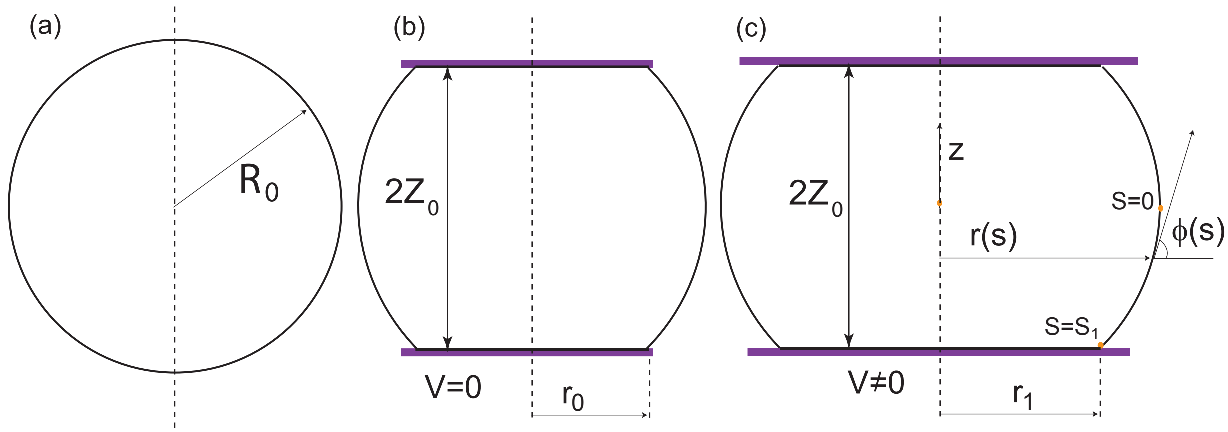

Figure 3: (a) The cell is a sphere of radius R_0 when it is not in contact with a substrate. (b) When it is brought in contact with a substrate at the top and bottom it becomes pancake shaped due to adhesive interactions. The geometry of the pancake is characterized by Z_0 and r_0, both of which depend on R_0 and the adhesion energy density Γ. (c) The force exerted by the cell on the substrate when $V \neq 0$ is determined by enforcing the constraint that Z_0 remains fixed even though the contact radius r_1 changes.

where $p = \frac{2\tau_0}{R_0}$. If we know τ_0, R_0, and r_0 then the parameter Γ can be estimated. Then Z_0 can be calculated from (27) and we can solve for F from (26). After carrying out these calculations we find that the equation for F is

$$Z_0 = R_0(1 - \frac{\Gamma}{\tau_0}) = \frac{\tau}{p}\left[\frac{1+\sqrt{1+\frac{Fp}{\pi\tau^2}}}{\sqrt{2}}\right]\left[1 - \frac{\frac{p^2r_1^2}{2\tau^2} - 1 - \frac{Fp}{2\pi\tau^2}}{\sqrt{1+\frac{Fp}{\pi\tau^2}}}\right]^{1/2}. \tag{30}$$

We can solve this equation for F using Newton's method. Unfortunately, a simple solution like the one in the previous section is difficult to obtain. In figure 4 we have plotted the solution for F using $R_0 = 10\mu$m and $r_0 = 0.85R_0$. It fits the data quite well and corresponds to $\frac{\Gamma}{pR_0} \approx 0.23$ which is in the regime where (28) is valid.

Cell off-center on the PZT beam

The cell contacts the PZT beam over a circular patch of radius r_1. Let us assume for simplicity that $r_1 << L$ where L is the length of the beam. In that case we can assume that the cell is exerting a point force F on the beam. Let this point force F act at $x = x_0$ with $0 < x_0 < L$ (see figure 5(a)). If the beam is clamped at both ends this leads to a deflection profile:

$$y(x|x_0) = \frac{F}{6EI}(1-\frac{x_0}{L})^2\left[x^3(1+\frac{2x_0}{L}) - 3x_0x^2\right] - \frac{F}{6EI}\langle x - x_0\rangle^3, \tag{31}$$

$$\frac{dy}{dx} = \frac{F}{2EI}(1-\frac{x_0}{L})^2\left[x^2(1+\frac{2x_0}{L}) - 2x_0x\right] - \frac{F}{2EI}\langle x - x_0\rangle^2. \tag{32}$$

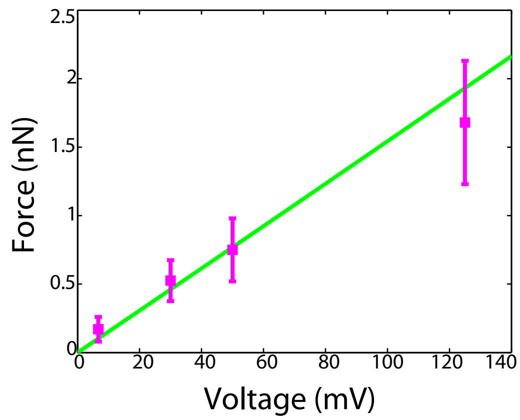

Figure 4: The experimental data (pink points) can be fit by theory even if we start with a pancake shaped cell. For this plot we have taken $R_0 = 10\mu$m and $r_0 = 0.85R_0$.

where $\langle x - x_0\rangle^n = 0$, if $x < x_0$ and $\langle x - x_0\rangle^n = (x - x_0)^n$, if $x \geq x_0$. The deflection $y(x_0|x_0)$ right under the load is given by

$$y(x_0|x_0) = -\frac{F}{3EIL^3}\left[x_0(L - x_0)\right]^3. \tag{33}$$

This deflection is zero when $x_0 = 0, L$ and maximum when $x_0 = \frac{L}{2}$. For a given F, if $x_0 = \frac{L}{2}$ the deflection $y(\frac{L}{2})$ is given by

$$y(\frac{L}{2}) = -\frac{FL^3}{192EI}. \tag{34}$$

We can now compute the ratio $\frac{y(x_0)}{y(\frac{L}{2})}$ as follows:

$$\frac{y(x_0|x_0)}{y(\frac{L}{2}|\frac{L}{2})} = 64\left[\frac{x_0}{L}(1 - \frac{x_0}{L})\right]^3. \tag{35}$$

In our experiments the PZT beams are calibrated so that a measured voltage gives us the force exerted by the cell on the PZT beam assuming that the cell is at $x = \frac{L}{2}$. If the cell is not at the center of the beam then the deflection of the beam will be smaller and the apparent force $F_{app} = \frac{192EIy(x_0|x_0)}{L^3}$. This is related to the actual F exerted by the cell as follows:

$$\frac{F_{app}}{F} = \frac{y(x_0|x_0)}{y(\frac{L}{2}|\frac{L}{2})} = 64\left[\frac{x_0}{L}(1 - \frac{x_0}{L})\right]^3. \tag{36}$$

E, I and L for the PZT beams are known but the deflections $y(x)$ are too small to measure accurately. The voltages produced by the beam deflections, however, can be accurately measured and give us F_{app}.

Let us now consider the case when the load F is not a point load but is distributed over a length $2z$ along the beam and centered at x_0. The load is uniformly distributed with intensity q, so that $2qz = F$ as shown in figure 5(b). In this case the deflection profile is given by:

$$y(x|x_0,z) = \frac{2qzx^3}{EIL}\left[(1-\frac{x_0}{L})^2(\frac{L}{2}+x_0)-\frac{z^2}{L^2}(\frac{L}{2}-x_0)\right]+\frac{qzx^2}{EIL}\left[z^2(\frac{2}{3}-\frac{x_0}{L})-\frac{x_0}{L}(L-x_0)^2\right]$$
$$-\frac{q}{24EI}\langle x-x_0+z\rangle^4+\frac{q}{24EI}\langle x-x_0-z\rangle^4. \quad (37)$$

Evaluating the deflection at the center point of the distributed load x_0, we get

$$y(x_0|x_0,z) = \frac{2qzx_0^2}{3EIL}(L-x_0)^2\left[\frac{z^2}{L^2}-\frac{x_0}{L}(1-\frac{x_0}{L})\right]-\frac{qz^4}{24EI}. \quad (38)$$

Note that as $z \to 0$ with $2qz = F$ we recover (33). To get an idea of how the distributed

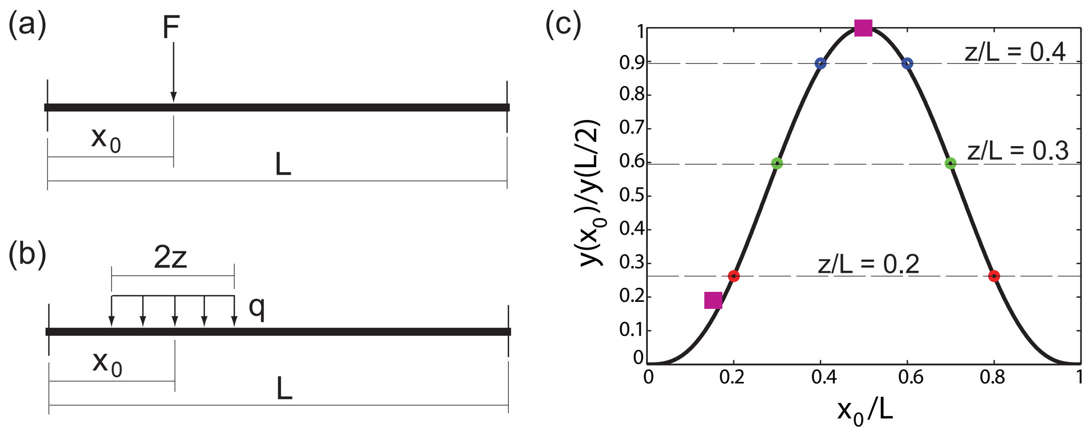

Figure 5: A cell exerts a distributed load q on a beam over a region of length $2z$ as shown in (b) with $2qz = F$. The center point of the distributed load is at x_0. $z = 0$ corresponds to a point load on the beam as shown in (a). We wish to compute the ratio of deflections $\frac{y(x_0)}{y(\frac{L}{2})}$ as a function of z and x_0. This is plotted in (c). The black curve corresponds to $z = 0$. For $z \neq 0$ the curve remains the same but the range over which $\frac{y(x_0)}{y(\frac{L}{2})}$ varies is smaller because the range of x_0 becomes $z \leq x_0 \leq L - z$. Using optical images we were able to observe a cell near $x/L = 0.15$ and another near $x/L = 0.5$. Recall that $\frac{y(x_0)}{y(\frac{L}{2})} = \frac{F_{app}}{F}$ from (36). For $x/L = 0.5$ we found $F_{app} = 1.7$nN and for $x/L = 0.15$ we got $F_{app} = 0.34$nN for the same amount of depolarization. These are plotted as magenta squares in (c) assuming $F = 1.7$nN. The point corresponding to $x/L = 0.15$ lies close to the theoretical curve.

load affects the deflection let us compute the ratio $\frac{y(x_0|x_0,z)}{y(\frac{L}{2}|\frac{L}{2},z)}$ which we will call $\frac{y(x_0)}{y(\frac{L}{2})}$ for compactness. This is given by

$$\frac{y(x_0|x_0,z)}{y(\frac{L}{2}|\frac{L}{2},z)} = \frac{16\left[\frac{x_0}{L}(1-\frac{x_0}{L})\right]^2\left[\frac{z^2}{L^2}-\frac{x_0}{L}(1-\frac{x_0}{L})\right]-\frac{z^3}{L^3}}{\left[\frac{z^2}{L^2}-\frac{1}{4}\right]-\frac{z^3}{L^3}} = \frac{y(x_0)}{y(\frac{L}{2})}. \quad (39)$$

This expression is plotted for $z = 0$ (corresponding to a point force) in figure 5(c) as the black curve. The range for $\frac{y(x_0)}{y(\frac{L}{2})}$ is $0 \leq \frac{y(x_0)}{y(\frac{L}{2})} \leq 1.0$ when $z = 0$. If the point of application of F is nearer to the ends than to the center then the deflection at x_0 is lesser than what it would be if F was acting at $\frac{L}{2}$. If $z \neq 0$ (corresponding to a distributed load q over a region $2z$) then the range for x_0 becomes $z \leq x_0 \leq L - z$ but the curve does not change. So, the conclusion that the beam deflection is maximum when $x_0 = \frac{L}{2}$ does not change. But, the range over which the deflection at x_0 varies decreases as z increases. In figure 5(c) the range for $\frac{y(x_0)}{y(\frac{L}{2})}$ is above the dashed horizontal line labeled $z/L = 0.3$ when $z = 0.3L - 0.6 \leq \frac{y(x_0)}{y(\frac{L}{2})} \leq 1.0$. This means that the error in computing the force exerted by the cell by just looking at the deflection at the center of the beam decreases as z increases.

References

[S1] Zhang, P.-C., Keleshian, A. M. and Sachs, F. Voltage-induced membrane movement. *Nature* **413**, 428-432, (2001).

[S2] Boal, D. H. *Mechanics of the cell*, Cambridge University Press, (2001).

[S3] Lin, Y. and Freund, L. B. Forced detachment of a vesicle in adhesive contact with a substrate. *Intl. J. Solids Struc.* **44**, 1927-1938, (2007).